Ann. Occup. Hyg., Vol. 56, No. 5, pp. 622–630, 2012

doi:10.1093/annhyg/mes005

Toxicity and Genotoxicity of Nano-SiO_2 on Human Epithelial Intestinal HT-29 Cell Line*

JACQUES-AURÉLIEN SERGENT†, VINCENT PAGET† and SYLVIE CHEVILLARD*

Laboratory of Experimental Cancerology, Institute of Cellular and Molecular Radiobiology, CEA, 92265 Fontenay-aux-Roses, France

Received 3 October 2011; in final form 12 December 2011; published online 29 February 2012

Silica mesoporous nanoparticles have been recently selected for a wide range of applications from electronics to medicine due to their intrinsic properties. Among medical applications, drug delivery using SiO_2 nanoparticles by oral route is under study. Major benefits are expected including higher specificity and sensitivity together with side effect reduction. Since literature shows that very complex and unexpected interactions could occur between nanomaterials and biological systems, one critical issue is to control the nanoparticle cytotoxicity/genotoxicity for normal tissues and specially stomach and intestine when oral route is considered. The aim of the work is to study the cytotoxicity and genotoxicity of SiO_2 nanoparticles on HT29 human intestine cell line, using conventional and innovative methodologies, for measuring cell viability and proliferation, global metabolism, genotoxicity, and nanoparticles uptake. Core-dye doped SiO_2 nanoparticles of 25 and 100 nm were specifically synthesized to track nanoparticles incorporation by confocal and video microscopy. Besides conventional approaches (sulforhodamine B, flow cytometry, and γ-H2Ax foci), we have performed a real-time monitoring of cell proliferation using an impedance-based system which ensure no interference between measures and nanoparticles physicochemical characteristics. Overall, our results showed that SiO_2-25nm and SiO_2-100nm induced a rather limited cytotoxic and genotoxic effects on HT-29 cells after a 24 h exposure. However, regarding cell viability and genotoxicity, inverse dose-dependant relationships were observed for SiO_2-100nm nanoparticles. In conclusion, it seems that the higher the dose of SiO_2-100nm, the lower the cytotoxic/genotoxic effects, data that well illustrate the complexity in identifying and understanding the hazards of nanoparticles for human health.

Keywords: cytotoxicity; flow cytometry; genotoxicity; HT-29; impedancemetry; nanoparticles; silica nanoparticle

INTRODUCTION

Environmental health (Kahru and Dubourguier, 2010), drug delivery, or biomedical engineering (Fadeel and Garcia-Bennett, 2010) are some of the promising fields for the application of nanotechnologies developed in the past decade (Clift *et al*., 2010). Furthermore, numerous studies have underlined particular characteristics of silica nanomaterials to improve the efficacy of therapeutic agents in tumor cells or as medical tools for biosensing and imaging (Wang *et al*., 2011). Despite intensive research efforts, reports of cellular responses to nanomaterials are often contradictory due to poorly characterized materials or unintended cross-reactions (Kurath and Maasen, 2006; Laaksonen *et al*., 2007; Ai *et al*., 2011). Toxicological data on the impact of SiO_2 nanoparticles on human intestinal cells *in vitro* and their detailed molecular mechanisms still remain unknown. Indeed, to our knowledge, there are no published data reporting the study of such nanoparticles upon biological human material from intestine, a major natural barrier

*Author to whom correspondence should be addressed.
Tel: +33 1 46 54 88 89; fax: +33 1 46 54 88 86;
e-mail: sylvie.chevillard@cea.fr
†These authors contributed equally to this work.
* *based on presentations at the INRS Symposium on Risks of Nanoparticles and Nanomaterials, Nancy, France, April 2011.*

of interest for oral administration. The aim of our study is to evaluate the potential toxicity of these nanoparticles on human HT-29 cell line.

We studied the proliferation of human intestinal cells exposed to nanoparticles using an impedancemetry-based innovative method (Xcelligence Roche) and the cytotoxicity of two SiO_2 nanoparticles (25 and 100 nm) via the conventional cytotoxicity assay sulforhodamine B (SRB), which evaluated global cell metabolism (Skehan *et al.*, 1990). Additionally, we have adapted two methods based on flow cytometry and confocal microscopy to study (i) cell mortality and (ii) DNA double-strand breaks by the detection of phosphorylated γ-H2AX-foci, together with the intracellular accumulation of nanoparticles (Paget *et al.*, 2011). In order to track the intracellular nanoparticles, we have exposed cells with SiO_2-25nm and SiO_2-100nm perfectly dispersed nanoparticles core-labeled with Rhodamine B and TMPyP, respectively, these two fluorophores being incorporated in mass during synthesis.

Interestingly, we have highlighted an inverse dose response for HT-29 cells exposed SiO_2-100nm particles, which well illustrates the complexity of nanomaterial hazard.

METHODS

Cell culture

Human HT-29 cells (ATCC number: HTB-38™, *TP53*-deficient/MMR-proficient) were routinely grown at 37°C in a humidified atmosphere of 5% CO_2 and 95% air, in Dulbecco's Modified Eagle Medium (DMEM) Glutamax supplemented with 10% (v/v) inactivated fetal bovine serum (FBS) and 1 mM Anti–Anti (Invitrogen). This medium is considered as complete DMEM.

Characterization of SiO_2 nanoparticles

Materials. Triton® X-100 (TX-100), Igepal CO-520, 1-hexanol anhydrous (≥99%), cyclohexane reagent plus® (≥99%), aqueous ammonia (NH_4OH) solution (25%), tetraethylorthosilicate (TEOS, 98%), ethanol, Rhodamine B, 5,10,15,20-tetrakis(1-methyl-4-pyridino)porphyrin tetra(toluene-4-sulfonate) (TMPyP) all purchased from Aldrich were used without further purification. Water was purified with a Milli-Q system (Millipore, Bedford, MA, USA) including a SynergyPak® unit. The exclusive Jetpore®, ultrapure grade mixed-bed ion-exchange resin, was also used in this unit. Water achieved resistivity >18.0 MΩ·cm at 25°C. A C 3.12 centrifuge (Jouan, France) and a Sonorex Digitec sonication water-bath (Roth, France) were used. Dialysis tubes have been purchased from Roth and possess a nominal filter rating of 3500 and an MWCO of 4000–6000 D.

Synthesis of SiO_2-25nm. Silica nanoparticles were synthesized using a reverse micro-emulsion method, as described by Bagwe *et al.* in the literature. In a 50 ml erlenmeyer, Igepal CO-520 (8 ml), cyclohexane (20 ml), and an aqueous solution or rhodamine B (650 µl at 0.01 M) were mixed and stirred at room temperature to form a homogeneous micro-emulsion. After 10 min of equilibration, aqueous ammonia NH_4OH (35 µl) was introduced in the micro-emulsion as the catalyst in the synthesis of the silica shell. After another 10 min of equilibration, TEOS (60 µl) was added. After a 24 h aging period, the nanoparticles were centrifuged (8000 g for 15 min) and washed several times with ethanol to remove unreacted and untrapped chemical species. Ultrasonification (35 Hz) was used in order to disperse nanoparticles aggregated into the washing solvent and to increase the desorption rate of surfactant from the surface of the synthesized nanoparticles. Then, the sample is subjected to dialysis against deionized water for a week.

Synthesis of SiO_2-100nm. Silica nanoparticles were synthesized using a reverse micro-emulsion method, as described by Tan *et al.* in the literature (Bagwe *et al.*, 2004). Consequently, a quaternary micro-emulsion consisted in mixing Triton X-100 (12.6 ml, 13.5 g, $d = 1.07$), 1-hexanol (12.3 ml), and cyclohexane (57 ml) under a vigorous stirring at room temperature, followed by additions of a concentrated aqueous solution of TMPyP dye in water (600 µl at 0.1 M), water (1.2 ml), aqueous ammonia NH_4OH (725 µl at 25%), and TEOS (725 µl) in that order. The mixture was allowed to stir for 24 h at room temperature and a subsequent addition of ethanol (100 ml) disrupted the inverse micelles. Particles were recovered by centrifugation (8000 g for 15 min) and washed thoroughly three times with ethanol and one time with water. Ultrasonification (35 Hz) was used in order to disperse nanoparticles aggregated into the washing solvent and to increase the desorption rate of surfactant from the surface of the synthesized nanoparticles. Then, the sample is subjected to dialysis in deionized water for a week. No trace of fluorophore alone was detected in the deionized water after dialysis, testifying their efficient in-mass incorporation.

Transmission electron microscopy. The morphologies and sizes of dye-doped silica nanoparticles were characterized using a transmission electron microscope (JEOL 2000 FX). The sample for transmission electron microscopy (TEM) were prepared by plunging a 200 mesh carbon-coated copper grid,

with a thickness of 30–50 nm, (Euromedex, France) in the desired nanoparticle-containing aqueous solution just after dispersion by ultrasonification. Further to the evaporation of the water, the particles were observed at an operating voltage of 200 kV. Once the samples were imaged, TEM micrographs of dye-doped silica nanoparticles were converted to digital images using imaging software (IMIX, PGT). Furthermore, elemental analysis of the samples could be performed by Energy Dispersion RX Spectroscopy (EDS).

Particle sizing. The hydrodynamic diameter and dispersivity of the silica nanoparticles were determined by Dynamic Light Scattering technique using a Zetasizer Nano ZS from Malvern Instruments. The light scattering measurements were performed using a 633 nm red laser in a back-scattering geometry ($\theta = 180°$). The particle size was analyzed using a dilute suspension of particles in deionized (or ultrapure) water and in complete culture media (containing 10% of FBS). Nanoparticles characterization are summarized in Table 1.

Fluorescence measurements. All fluorescence measurements were performed at room temperature on a steady-state FS920 spectrofluorimeter (Edinburgh Instruments, UK) with a high spectral resolution (signal to noise ratio $>$ 6000:1), using water as the solvent, and a 1-cm cell, the latter oriented at $-45°$ to the direction of the excitation light beam. The spectrofluorimeter covers the wavelength range from 200 to 1670 nm using two detectors: a photomultiplier R928 for UV–Vis scans (up to 870 nm) and a solid InGas TE G8605-23 detector for infrared scans. The excitation source is a continuous Xenon Arc lamp (450 W) coupled to two Czerny-Turner DMX300X 1800 tr/mn monochromators, one for UV excitation (focal length 300 mm) and one for visible wavelength (focal length 500 mm). Fluorescence intensity values were integrated over the wavelength region specified. Data were recorded in a comparative manner, approximately using the same aperture of slits.

Xcelligence. Background of the E-plates (Roche Diagnostics) was determined in 100 µl of medium and subsequently 100 µl of the HT-29 cell suspension was added (15 000 cells per well). Cells were incubated for 30 min at 37°C and E-plates were placed into the Real-Time Cell Analyzer (RTCA) station (Roche Diagnostics). Cells were grown for at least 24 h, with impedance measured every 5 min during 6 h (adhesion phase), then every 15 min (proliferation phase). After at least 24 h cells were exposed to SiO_2-25nm and 100nm at concentrations from 10, 25, 50, 75, and 150 µg ml^{-1} and were monitored again every 5 min during 6 h (early effects), then every 10 min until the end of experiment (late effects). Cell index (CI) raw data values are calculated as follows: $Zi - Z0\ [\Omega]/15[\Omega]$; where Z0: is the background resistance and Zi: the individual time point resistance. Normalized cell index are also calculated by the software at the selected normalization time point (nml_time), which was chosen as time just before the addition of nanoparticles.

Cytotoxicity

HT-29 human cells were exposed to SiO_2-25nm and -100nm at concentrations of 0, 10, 50, and 150 µg ml^{-1} for 24 h at 37°C in 96-well microplates. Cytotoxicity was evaluated using SRB assay (Sigma) according to the Skehan protocol (Skehan *et al.*, 1990).

Flow cytometry

After 24 h treatments, cells were washed and trypsinized for 5 min. Trypsine was inactivated by complete DMEM, cells were centrifuged for 5 min at 300 g and then resuspended in 500 µl of DMEM with serum in flow cytometry compatible tubes (BD 352058). Multi-parametric analyses were performed on BD Facscalibur using FlowJo 7.5.5 software. A first analysis was realized on size/granulometry to collect living and dead cells and to remove fragmented cells. Rhodamine-doped SiO_2-25nm nanoparticles events are then collected on FL2 (585/42 nm) and TMPyP-doped SiO_2-100nm on FL3 ($>$670 nm), respectively, corresponding to both optimal fluorescence emission after Argon Ion excitation at 488 nm. To-Pro3 (Molecular Probes, Invitrogen) signal was collected on FL4 (λ_{em}: 661/16 nm) after He-Ne laser excitation at 636 nm and was used for the analysis of cell viability since this dye is compatible without interference with equipment and nanoparticles detection. The results are reported as the mean distribution of cell fluorescence, obtained on three replicas with at least 15 000 events per replica. Measurements are given on a bi-parametric representation divided in quarters and are associated to four different cell populations: living cells without nanoparticles (ToPro3/Nanoparticles negative cells), living cells with nanoparticles (ToPro3 negative/Nanoparticles positive cells), dead cells with nanoparticles (ToPro3 positive/Nanoparticles positive cells), and dead cells without nanoparticles (ToPro3/Nanoparticles positive cells).

Genotoxicity

Phosphorylated-γ-H2Ax-foci. Thirty thousand cells were seeded on Lab-Tek™ II Chamber Slide™ eight wells (Nunc) 24 h before exposure and cells were treated for 24 h with nanoparticles at doses of 10, 50, and 150 µg ml^{-1}. After treatment, cells were washed and

fixed for 15 min with paraformaldehyde 4%, washed twice with 200 µl of 1× phosphate-buffered saline (PBS) and then permeabilized for 10 min at room temperature in [1× PBS and Triton 0.1%]. We labeled nuclei with Hoechst 33342 (λ_{ex}: 350 nm, λ_{em}: 461 nm) and γ-H2Ax with Alexa Fluor® 488 (λ_{ex}: 495 nm, λ_{em}: 519 nm). Cells were blocked in [1× PBS, 0.025%, 10% of goat serum (Jackson ImmunoResearch)] for 1 h at room temperature, then incubated for 75 min at room temperature with 1:500 of monoclonal γ-H2Ax antibody (Anti-phospho-Histone H2Ax (Ser139), clone JBW301, 05-636, Upstate Millipore), washed with 3 × 300 µl of [1× PBS, Triton 0.025%] and then incubated at room temperature for 45 min with 1:500 dilution of Alexa Fluor® 488 goat anti-mouse IgG (H + L) (Molecular Probes, Invitrogen) as a secondary antibody. Samples were washed with 3 × 300 µl of [1× PBS, Triton 0.025%] and cells were incubated at 37°C for 20 min with 200 µl of [1× PBS and Hoechst 33342 at 0.1 µg ml^{-1} (Molecular Probes, Invitrogen)]. Finally, Lab-Tek™ Chamber Slide™ eight wells were washed with 3 × 300 µl of [1× PBS, Triton 0.025%] before mounting in ProLong® Gold antifade reagent (Molecular Probes, Invitrogen) in order to proceed for confocal microscopy visualization.

Confocal microscopy. Fixed and labeled cells were photographed with an ACS APO 40X oil CS (NA 1.15) objective under a fluorescence confocal microscope (Leica TCS SPE, Wetzlar, Germany) equipped with four diode lasers (405, 488, 532, and 635 nm). The spectral sliders were set in sequential mode and by decreasing excitation wavelengths, to maximize signal and to reduce spectral overlap. All the details concerning the proceedings of the acquisitions are reported in Table 2B. Each analysis was made on at least 100 cells and at least six images of each condition were analyzed. Confocal microscopy optical slice sections of 8–20 µm were made from the luminal to the basal pole of the cells, each acquisition containing nine stacks. Images were prepared and stacked with ImageJ software (Abramoff *et al.*, 2004) by using the stacks tool. Then, the tiff images were converted into 8 bits before performing foci counts. Cell Profiler software (Carpenter *et al.*, 2006) was used for the detection and scoring of foci in Alexa Fluor images.

Statistical analysis. To test whether the basal number of γ-H2Ax-foci observed in control cells was significantly different from that observed in nanoparticles exposed cells, a Wilcoxon rank test based on at least 100 observations for each condition was performed.

Table 1. Summarized characterization of silica mesoporous nanoparticles used.

	SiO_2-25nm	SiO_2-100nm
Produced raw materials		
TEM diameters (nm)	20 ± 3	90 ± 5
Core dye-doped fluorophore used	Rhodamine B	TMPyP
Theoretical fluorophore $\lambda_{ex}/\lambda_{em}$	557/578	405/(670–714)
Nanoparticles $\lambda_{ex}/\lambda_{em}$	556/580	428/(668–718)
Dispersed nanomaterials		
Dynamic light scattering in deionized water	22 ± 5	97 ± 7
Dynamic light scattering in complete DMEM (after 24 h)	25 ± 5	95 ± 5

Table 2. Dyes characteristics (A) and settings parameters used for confocal microscopy (B). Ordering of sets and conditions were used for confocal acquisitions.

A. Characteristics of the dyes used in this study

Dye	Staining	λ_{ex} (nm)	λ_{em} (nm)
Hoeschst 33342	Nucleus	350	461
Alexa Fluor 488	γ-H2Ax	495	519

B. Ordering of sets and conditions used for confocal acquisitions

Set number	Dye	Staining	Laser used (nm)	Wavelengths gathering used (nm)	Laser power used (%) (upon the 2 mW (theoretical max.) delivered by the system)
1	Alexa Fluor 488	γ-H2Ax	488	500–540	16
2	Hoeschst 33342	Nucleus	405	410–470	9

RESULTS

Xcelligence profile (impedancemetry)

Xcelligence is a method based on impedancemetry to assess the global resistance of adherent cells using a cell Index (CI) metric (Vistejnova *et al.*, 2009; Ke *et al.*, 2011). Variation of CI reflects either variation in cell number or cell morphology and membrane integrity. An example of CI variation of exponentially growing of control cells is shown in black on Fig. 1. With 15 000 cells initially seeded, the mean doubling time is ∼22 h, which is consistent with what is known for HT-29 cell proliferation (Forgue-Lafitte *et al.*, 1989). Before nanoparticle exposure, untreated cells are monitored for at least 24 h for controlling adhesion and proliferation. Then, cell index was standardized (time 0) when nanoparticles are added to cell culture. As seen in Fig. 1, overall SiO_2-25nm are not cytotoxic, cell growth is quite similar to that of control cells, except during the first 24 h during which a slightly slower growth rate is observed. By contrast, HT-29 cells exposed to SiO_2-100nm nanoparticles show an inverse relationship between CI and dose: the lowest dose being more cytotoxic than the highest dose (Fig. 1).

Cytotoxicity

Cytotoxicity was also evaluated using the sulforhodamine B test that measures global metabolism activity (Skehan *et al.*, 1990). Data obtained after 24 h of exposure to various doses of SiO_2-25nm or SiO_2-100nm indicate that the global metabolism is not altered (Fig. 2).

Flow cytometry measurement of nanoparticles incorporation and cell viability after 24 h of exposure to nano-SiO_2

After adding the cell viability reporter ToPro3, a bi-parametric analysis permits the detection of intracellular nanoparticles together with the discrimination of viable and dead cells (Fig. 3). An example of flow cytometry analysis is given in Fig. 3A for control cells, Fig. 3B for exposed cells to 25 and 100 nm nanoparticles and data are summarized in Fig. 3C.

Again, a limited cytotoxicity is observed for SiO_2-25nm for doses ranged from 10 to 150 μg ml^{-1}, the dead population is increasing from 5 to 15% of the population at the higher dose (Fig. 3C). Flow cytometry measurement of cell mortality confirmed the

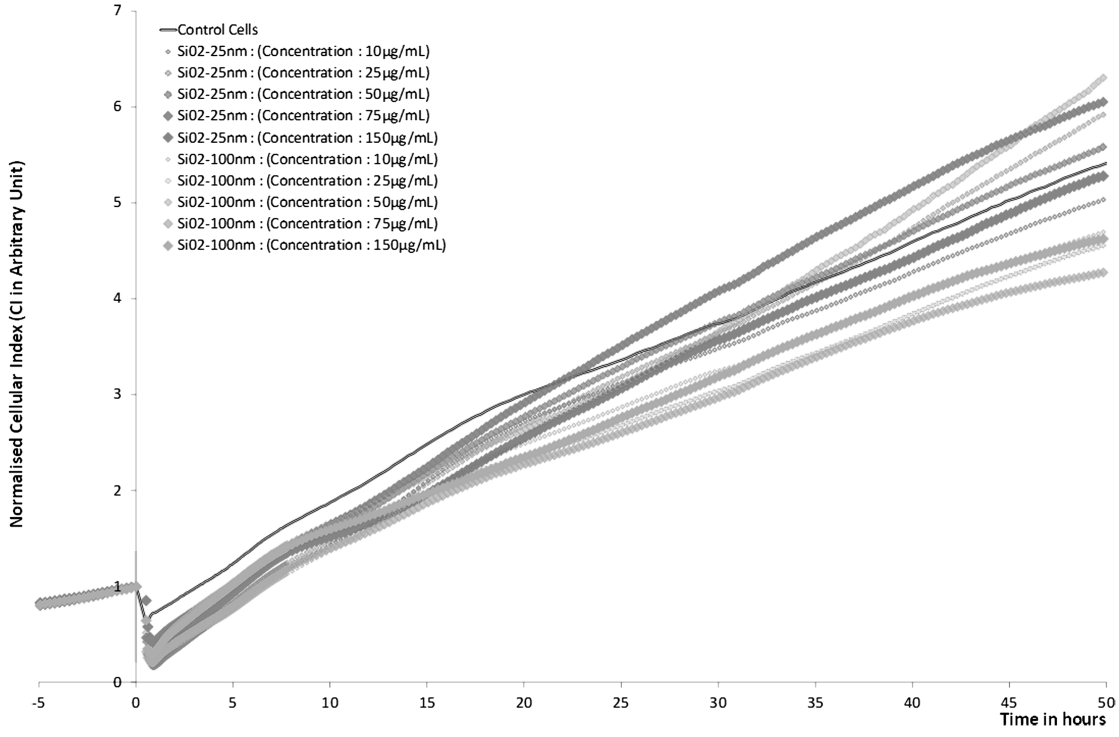

Fig. 1. Cell index real-time monitoring of HT-29 cells non-exposed (in black) and exposed to 10, 50, 150 μg ml^{-1} of SiO_2-25nm (in red) and SiO_2-100nm (in green) for 48 h. Time 0 represents the addition of the nanoparticles. Cell index were normalized at Time 0 to ensure non inter-wells variability prior to the addition of nanoparticles.

inverse relationship between doses of SiO_2-100nm and cell death; the lower the dose the higher the mortality. Twenty-four hours after SiO_2-100 mm exposure, cell death ranges from 40 to 15% for 10 and 150 μg ml^{-1}, respectively. However the proportion of living and dead cells, which have incorporated nanoparticles, increases as function of the dose, with a maximum of intracellular nanoparticles for the higher dose.

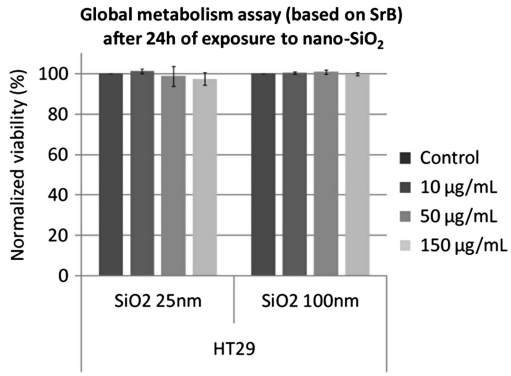

Fig. 2. Global metabolism activity of HT-29 cells performed by sulforhodamine B (SRB) assay after a 24 h contact with SiO_2-25nm or SiO_2-100nm nanoparticles. Non-exposed cells were normalized to 100%.

Genotoxicity

γ-H2Ax phosphorylation and recruitment under foci pattern is associated to double-strand DNA breaks (Rogakou *et al.*, 1998). The overall distribution of γ-H2Ax foci and median values are faintly significantly different in cell exposed to SiO_2-25nm compared to control cells except for the higher dose, for which a decreased distribution with the same median value is observed, suggesting a higher number of foci per nucleus (Fig. 4). For SiO_2-25nm nanoparticles, γ-H2Ax-foci per nucleus median values are not significantly different to that of control cells, except for the higher dose (13, 12, and 13.5 for 10, 50, and 150 μg ml^{-1}, respectively) (Fig. 4). Regarding data obtained with SiO_2-100nm, as for cytotoxicity, it seems that lower is the dose higher is the genotoxicity. γ-H2Ax-foci per nucleus median values are significantly different to that of control cells, except for the highest dose (16, and 11 for 10, 50, and 150 μg ml^{-1}, respectively).

DISCUSSION

In this study, we explored the cytotoxicity and genotoxicity of nano-SiO_2 on HT-29 cells, deriving from a colorectal adenocarcimona, which are

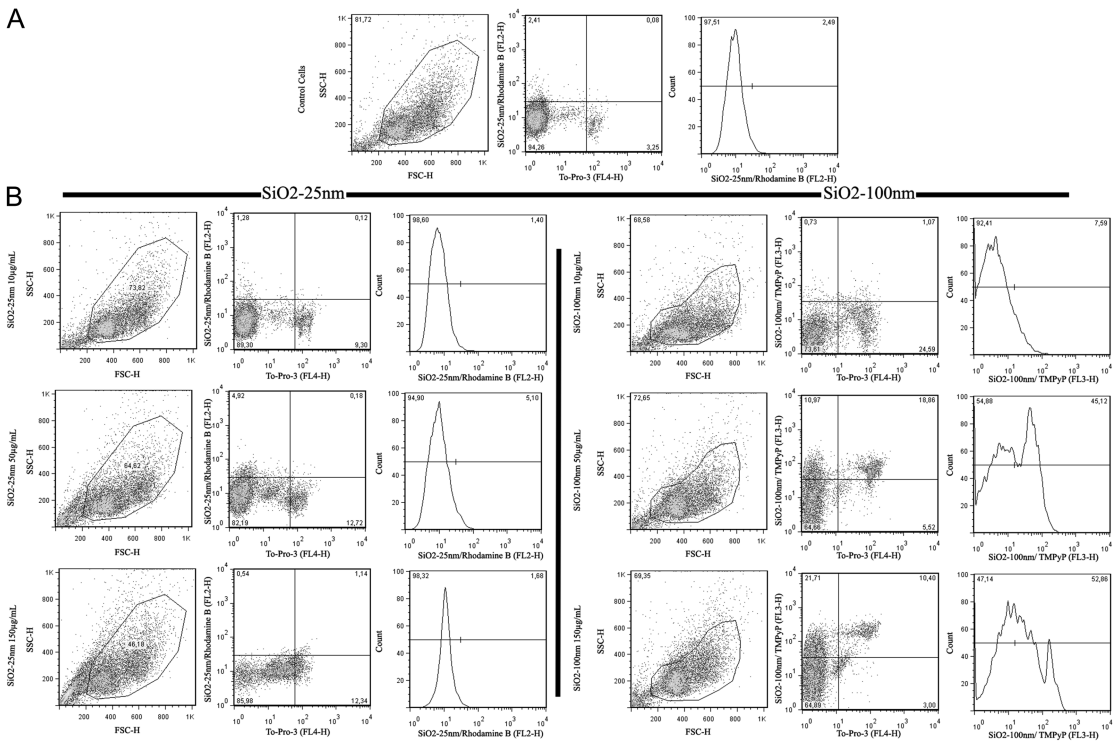

Fig. 3. Continued.

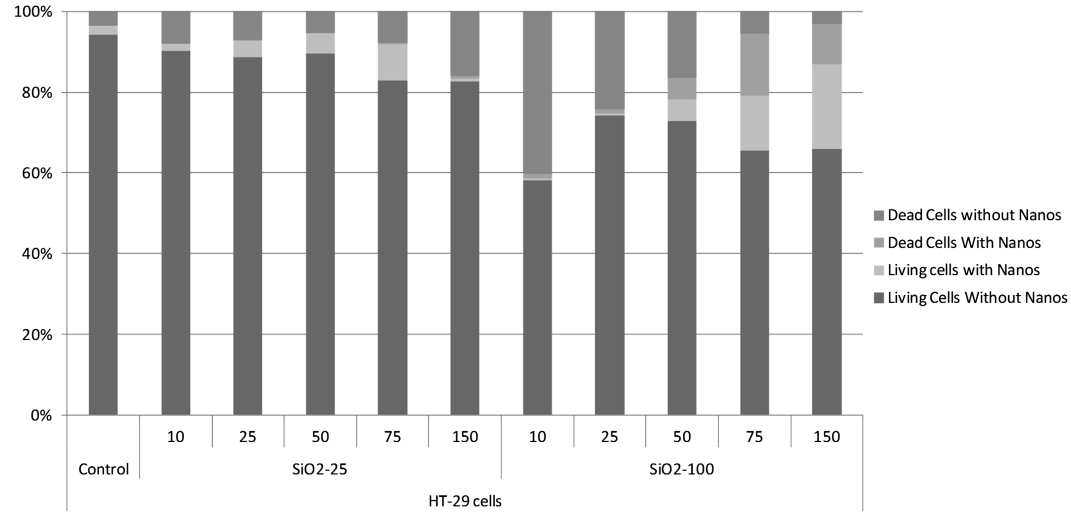

Fig. 3. Flow cytometry analysis of nano-SiO_2 incorporation and HT-29 cell viability after a 24 h exposure. Bi-parametric analysis was performed to correlate ToPro3 incorporation (as a living/dead cells reporter) and nanoparticle fluororeporter (rhodamine B for SiO_2-25nm and TMPyP for SiO_2-100nm nanoparticles): control cells (A), nanoparticles-exposed cells (B). Summarized data are reported in (C) for three independent experiments based on 15 000 gated cells with morphology similar to that of control cells.

representative of the intestinal membrane. Like the Caco-2 cell line, the HT-29 cells are typical of intestinal compartment (Rousset, 1986) and both are polarizable cells (Le Bivic *et al.*, 1988). SiO_2 nanoparticles may be widely used in agro-alimentary industries or for drug delivery in the foreground future.

Numerous studies described potential toxicity of SiO_2 nanoparticles on cell lines but many are controversial due to lacking information on nanoparticles synthesis, dispersion, and/or its stability in biological media. In this study, all experiments were realized using the same batch of nanoparticles just after synthesis, a 1-week dialysis, and monodispersed suspension in culture media. In these conditions, SiO_2-25nm and -100nm were both stable for at least 24 h as previously described (Paget *et al.*, 2011).

The global proliferation assay, based on impedancemetry of adherent cells due to low alternative current recording, allows to assess nanoparticles toxicology without any interferences in the measurements, such as for example cell trypzination. It is specifically important when dealing with nanoparticles since several studies have already reported interferences due to the presence of nanoparticles in several conventional colorimetric assays used in toxicology. Indeed, we have ensured that nanoparticles do not interact to the measurement of impedancemetry. For the highest tested concentration of nanoparticles (150 μg ml^{-1}), the CI measured in wells free of cells was closed to 0 during the whole experiment, testifying the absence of interferences from nanoparticles. Overall, SiO_2-25nm is not cytototxic for HT29 cells as illustrated by the rather constant CI, the absence of cell mortality and of modification of global metabolism. At the opposite, SiO_2-100nm seems to induce more effects than SiO_2-25nm but surprisingly with an inverse relationship with the dose. This unusual tendency was observed with the CI and was confirmed by the number of DNA double strand breaks and by cell mortality, which are higher at the lower dose. On the other, the SRB assay did not show any significant difference compared to non-exposed cells. It could be explained by modification of HT29 cells morphology due to exposure to SiO_2-100nm nanoparticles, while such phenomenon is detected by XCelligence system and is integrated in the calculation of the CI. These data are not related to the intracellular accumulation of nanoparticles since after exposure with the higher dose of SiO_2-100nm 20% of living cells contain nanoparticles, while only few percent of cells treated with the lower dose contain nanoparticles (Fig. 3C). Interestingly, SiO_2-100nm induced genotoxicity in HT29 cells, as seen by the higher number of γ-H2AX foci as compared to control cells except after the highest 150 μg ml^{-1} dose. Overall, it seems that SiO_2-100nm is more cytotoxic and genotoxic than SiO_2-25nm, but with an inverse relationship between effects and dose. This unusual effect may be explained by a biological protective process that could take place depending on the level of toxicity or damages within the cells specifically in HT29 cell line since it was not observed on human kidney

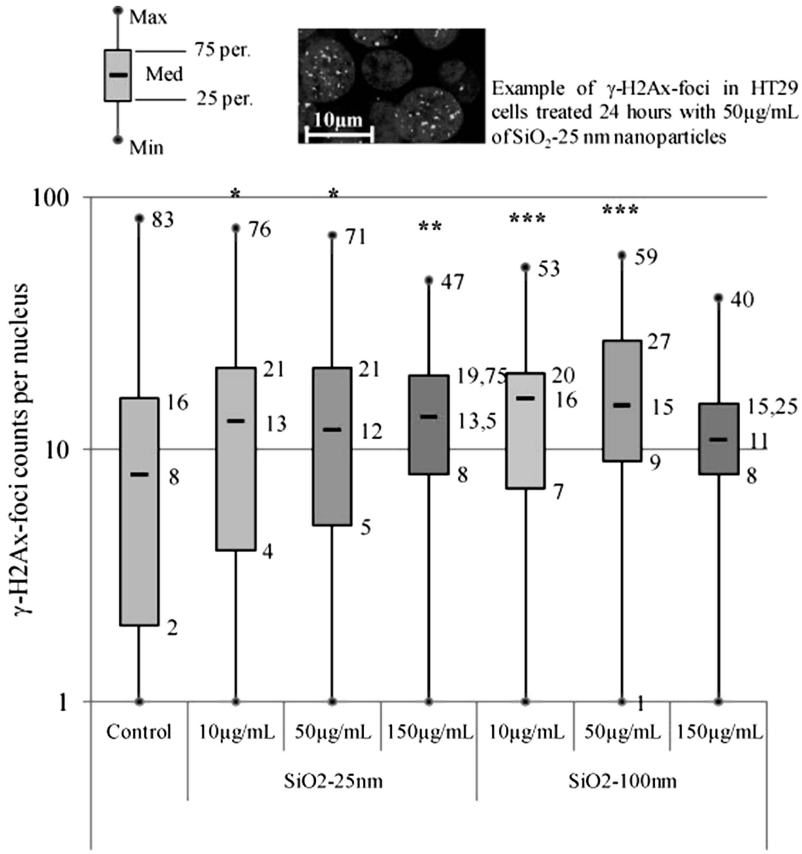

Fig. 4. Genotoxicity of SiO_2 on HT-29 cells measured by phosphorylated γ-H2AX foci per nucleus after a 24 h exposure. An example of positive staining is shown. Each rod corresponds for at least 100 cells, to the maximum, 75th percentile, median, 25th percentile, and minimum values for phosphorylated γ-H2Ax count per nucleus. Statistical analysis was done using a Wilcoxon rank test ($*P < 0.05$, $**P < 0.01$, $***P < 0.001$).

cell lines (Paget *et al.*, 2011). In this respect, it was shown that HT-29 cells are more efficient to repair DNA than normal colonocytes (Rosignoli *et al.*, 2001) but more importantly, a phenomenon of phagocytosis of damaged cells by non damaged cells could occur to maintain the islet profile integrity (Polak-Charcon and Ben-Shaul, 1979). This phenomenon could also explain the greater proportion of SiO_2-100nm in living cells after exposure at the highest dose.

FUNDING

NanoSciences CEA-Transverse program; C'Nano Ile-de-France: AI2009-FIN_31 Nanomique.

Acknowledgements—The authors thank Aurélien Auger from the CEA-Grenoble for providing core dye-doped nanoparticles and Thierry Kortulewski from the microscopy facility at CEA-IRCM institute for his technical advice.

REFERENCES

Abramoff MD, Magalhaes PJ, Ram SJ. (2004) Image Processing with ImageJ. Biophotonics Int; 11: 36–42.

Ai J, Biazar E, Jafarpour M *et al.* (2011) Nanotoxicology and nanoparticle safety in biomedical designs. Int J Nanomedicine; 6: 1117–27.

Bagwe RP, Yang C, Hilliard LR *et al.* (2004) Optimization of dye-doped silica nanoparticles prepared using a reverse microemulsion method. Langmuir; 20: 8336–42.

Carpenter AE, Jones TR, Lamprecht MR *et al.* (2006) CellProfiler: image analysis software for identifying and quantifying cell phenotypes. Genome Biol; 7: R100.

Clift MJ, Gehr P, Rothen-Rutishauser B. (2010) Nanotoxicology: a perspective and discussion of whether or not in vitro testing is a valid alternative. Arch Toxicol; 85: 723–31.

Fadeel B, Garcia-Bennett AE. (2010) Better safe than sorry: understanding the toxicological properties of inorganic nanoparticles manufactured for biomedical applications. Adv Drug Deliv Rev; 62: 362–74.

Forgue-Lafitte ME, Coudray AM, Bréant B *et al.* (1989) Proliferation of the human colon carcinoma cell line HT29: autocrine growth and deregulated expression of the c-myc oncogene. Cancer Res; 49: 6566–71.

Kahru A, Dubourguier HC. (2010) From ecotoxicology to nanoecotoxicology. Toxicology; 269: 105–19.

Ke N, Wang X, Xu X *et al*. (2011) The xCELLigence system for real-time and label-free monitoring of cell viability. Methods Mol Biol; 740: 33–43.

Kurath M, Maasen S. (2006) Toxicology as a nanoscience?—disciplinary identities reconsidered. Part Fibre Toxicol; 3: 6.

Laaksonen T, Santos H, Vihola H *et al*. (2007) Failure of MTT as a toxicity testing agent for mesoporous silicon microparticles. Chem Res Toxicol; 20: 1913–18.

Le Bivic A, Hirn M, Reggio H. (1988) HT-29 cells are an in vitro model for the generation of cell polarity in epithelia during embryonic differentiation. Proc Natl Acad Sci U S A; 85: 136–40.

Paget V, Sergent JA, Chevillard S. (2011) Nano-silicon dioxide toxicological characterization on two human kidney cell lines. J Phys: Conf Ser; 304: 012080.

Polak-Charcon S, Ben-Shaul Y. (1979) Degradation of tight junctions in HT29, a human colon adenocarcinoma cell line. J Cell Sci; 35: 393–402.

Rogakou EP, Pilch DR, Orr AH *et al*. (1998) DNA double-stranded breaks induce histone H2AX phosphorylation on serine 139. J Biol Chem; 273: 5858–68.

Rosignoli P, Fabiani R, De Bartolomeo A *et al*. (2001) Protective activity of butyrate on hydrogen peroxide-induced DNA damage in isolated human colonocytes and HT29 tumour cells. Carcinogenesis; 22: 1675–80.

Rousset M. (1986) The human colon carcinoma cell lines HT-29 and Caco-2: two in vitro models for the study of intestinal differentiation. Biochimie; 68: 1035–40.

Skehan P, Storeng R, Scudiero D *et al*. (1990) New colorimetric cytotoxicity assay for anticancer-drug screening. J Natl Cancer Inst; 82: 1107–12.

Vistejnova L, Dvorakova J, Hasova M *et al*. (2009) The comparison of impedance-based method of cell proliferation monitoring with commonly used metabolic-based techniques. Neuro Endocrinol Lett; 30 (Suppl 1): 121–7.

Wang TT, Chai F, Wang CG *et al*. (2011) Fluorescent hollow/rattle-type mesoporous Au@SiO2 nanocapsules for drug delivery and fluorescence imaging of cancer cells. J Colloid Interface Sci; 358: 109–15.